THE ASTROPHYSICAL JOURNAL, 250:43–54, 1981 November 1

VELOCITY DISPERSIONS IN THE BULGES OF SPIRAL AND S0 GALAXIES. II. FURTHER OBSERVATIONS AND A SIMPLE THREE-COMPONENT MODEL FOR SPIRAL GALAXIES

BRADLEY C. WHITMORE AND ROBERT P. KIRSHNER[1]
Department of Astronomy, University of Michigan
Received 1980 December 1; accepted 1981 May 4

ABSTRACT

We have obtained velocity dispersions for 24 galaxies in the Virgo cluster to supplement our earlier results. A 2000 channel intensified Reticon scanner has again been used on the 1.3 m telescope of McGraw-Hill Observatory, and a Fourier quotient technique has been employed to yield dispersions. We have confirmed our earlier result that spiral bulges exhibit a relation between total luminosity and velocity dispersion with the form $L \propto \sigma^4$, but with velocity dispersions that are $17 \pm 8\%$ smaller than elliptical galaxies at the same absolute magnitude. However, possible systematic errors may still affect the reality of this gap. The scatter in the $L \propto \sigma^4$ relationship is substantially larger for the spiral bulges than for the elliptical galaxies. This larger scatter probably indicates that spiral bulges comprise a more heterogeneous sample than do elliptical galaxies. We also find that the bulge components of S0 galaxies follow a $L \propto \sigma^4$ relation with no gap with the ellipticals. The similarity in this relation for the spheroidal components of spiral, S0, and elliptical galaxies indicates that the systems are dynamically similar.

We have compared our velocity dispersions with rotational velocities determined from neutral hydrogen widths. For a totally bulge dominated spiral the ratio of the asymptotic rotational velocity to the velocity dispersion is about 1.4. This suggests that the mass responsible for producing the flat rotation curves (presumably the "halo") resides in a spheroidal component rather than in the disk. Our study also substantiates our earlier result that the massive halo is not merely an extension of the bulge, but is a separate dynamical component for most of our galaxies. A simple three-component model has been constructed to aid in the interpretation of this data. These models provide an independent indication of the existence of massive halos in spiral galaxies.

Subject headings: galaxies: internal motions — galaxies: nuclei — galaxies: structure

I. INTRODUCTION

In a previous paper (Whitmore, Kirshner, and Schechter 1979, hereafter WKS) we reported the measurement of central velocity dispersions in 30 galaxies, 21 of which were spirals. We found that the spheroidal bulges of spiral galaxies obey the same $L \propto \sigma^4$ relation between luminosity and velocity dispersion that has been found in elliptical galaxies (Faber and Jackson 1976). However, the dispersions in the spiral bulges averaged 15% less than in ellipticals at the same absolute magnitude. We also compared circular velocities with our central velocity dispersions. This showed that the bulge and the unseen halo must be separate dynamical components, with a smaller velocity dispersion in the bulge than in the halo.

The analysis in WKS was limited by the lack of a consistent set of surface photometry and rotational velocities for our sample. We have attempted to alleviate this problem in the present study by supplementing our sample with measurements of velocity dispersions for 24 galaxies in the Virgo cluster. Fraser (1977) has obtained luminosity profiles for most of these galaxies. We have also obtained velocity dispersions for enough S0 galaxies to begin studying these systems. A simple three-component model has been constructed to aid in the interpretation of the comparison of our velocity dispersions with circular velocities. This model consists of the superposition of a bulge (King model), an exponential disk, and a dark isothermal halo.

II. OBSERVATIONS AND REDUCTIONS

The observations were made using a 2000 channel intensified Reticon scanner on the 1.3 m telescope at McGraw-Hill Observatory. The observing procedure was essentially identical to the technique described in WKS. The slit was 3″ × 10″, aligned along the minor axis to minimize rotational smearing.

Velocity dispersions were determined using the Fourier quotient method developed by Paul Schechter and described in Sargent *et al.* (1977). This method simultaneously solves for the velocity dispersion σ, the redshift z, and a line strength index γ. The bin size was 46 km s^{-1} for the majority of the spectra. A few high dispersion spectra were obtained at 22 km s^{-1} bin^{-1}. The resulting FWHM for comparison lines were 270 km s^{-1} and 140 km s^{-1}. In WKS we found that equation (1) was needed to correct

[1] Alfred P. Sloan Research Fellow.

TABLE 1

VELOCITY DISPERSIONS, MAGNITUDES, AND DISTANCES

NGC	Type	Velocity Dispersion (km s^{-1})		Absolute Magnitude	Bulge Magnitude, Rating	Distance (Mpc)	γ	Source of Photometry
224	Sb	151 ± 16		−20.37	−19.00, 1	0.69	...	e
3031	Sab	157 ± 17[b]		−20.09	−19.41, 3	3.2	...	f
3351	SBb	101 ± 16[b]		−20.59	−18.14, 2	14.8	...	g
4192	Sab	118 ± 17	128 ± 18	−21.06	−19.26, 2	22.0	0.59	h
		138 ± 18[a]						
4216	Sb	239 ± 16		−21.01	−20.01, 1	22.0	0.86	h
4254	Sc	157 ± 27[b]		−21.50	−19.34, 3	22.0	...	h
4303	Sbc	102 ± 19	96 ± 19	−22.02	−19.84, 1	25.4	0.61	h
		91 ± 19[a]						
4321	Sbc	91 ± 23		−21.82	−19.69, 1	22.0	0.44	h
4378	Sa	164 ± 20		−19.95		25.4	...	
4394	SBb	141 ± 16		−20.18	−19.05, 2	22.0	0.73	h
4450	Sab	101 ± 16	116 ± 16	−21.03	−19.85, 1	22.0	0.68	h
		130 ± 17[b]						
4501	Sb	159 ± 22[b]		−21.65	−19.54, 1	22.0		h
4548	SBb	155 ± 14		−20.94	−19.27, 1	22.0	0.84	h
4565	Sb	116 ± 17		−21.28	−20.28, 2	18.9	0.70	i
4579	Sb	187 ± 17	191 ± 18	−21.31	−20.40, 2	22.0	0.58	h
		195 ± 20[b]						
4594	Sa	263 ± 32[b]		−23.08	−22.86, 1	26.1	...	i
4698	Sab	172 ± 16		−20.53	−19.60, 1	22.0	0.74	h
5457	Scd	80 ± 20[b]		−22.06	−17.97, 2	10.2	...	f
7217	Sab	185 ± 18[b]		−21.44	−20.74, 2	24.5[d]	...	i
7331	Sbc	176 ± 18[b]		−21.93	−21.70, 1	22.1[d]	j	...
3377	E5	186 ± 21[b]		−20.03	...	14.8	...	
3379	E1	268 ± 24[b]	246 ± 23	−20.88	...	14.8		
		224 ± 22[a, b]						
4374	E1	301 ± 23		−21.61	...	22.0	0.72	
		262 ± 38[b]	282 ± 30					
		284 ± 28[a, b]						
4387	E5	165 ± 17		−18.97	...	22.0	0.77	
4406	E3	283 ± 18		−21.81	...	22.0	0.81	
4472	E2	286 ± 18		−22.61	...	22.0	0.87	
		301 ± 25[b]	300 ± 23					
		312 ± 26[a]						
4478	E2	127 ± 14		−19.79	...	22.0	0.76	
4486	E0	358 ± 29		−22.36	...	22.0	0.80	
4551	E3	132 ± 14		−19.07	...	22.0	0.73	
3115	S0	295 ± 17[b]		−20.18	−19.99	9.5[d]	...	k
3384	S0	200 ± 19[b]		−20.22	−19.64	14.8	...	l
3412	S0	97 ± 13[a, b]	104 ± 14	−19.64	−19.14	14.8	...	m
		111 ± 14[b]						
3489	S0	146 ± 10[b]		−19.45	−18.95	11.8	...	m
4203	S0	182 ± 14		−20.17	−18.98	18.9	0.81	l
4382	S0	186 ± 16		−21.82	−21.57	22.0	0.80	l
4442	S0	252 ± 19		−20.63	−20.13	22.0	...	m
4459	S0	163 ± 18		−20.57	−20.37	22.0	0.74	l
Preliminary results of Observations from Mount Hopkins Observatory								
474	S0/a	170		−21.58	...	46.7		
488	Sb	234		−22.44	...	46.7		
524	S0	237		−22.10	−21.60	46.7		m
613	Sbc	126[c]		−21.74	...	29.2[d]		
628	Sc	60[c]		−21.53	...	15.9[d]		
681	Sab	139		−20.46	...	38.6		
936	S0	191		−21.55	−21.05	30.3		m
949	Sb	68[c]		−18.97	...	15.7[d]		
1023	S0	211		−20.87	−20.37	12.4		m
1084	Sc	92[c]		−21.42	...	30.3		
1358	S0/a	161		...	...	...		
2217	S0	235		−22.01	−21.51	36.5		m
2336	Sbc	141		−22.67	...	47.8[d]		
2681	S0/a	105[c]		−19.57	...	11.8		
2683	Sb	143		−18.19	...	4.8[d]		
2775	Sab	183		−20.59	...	19.3[d]		

TABLE 1—*Continued*

NGC	Type	Velocity Dispersion (km s^{-1})	Absolute Magnitude	Bulge Magnitude, Rating	Distance (Mpc)	γ	Source of Photometry
2841	Sb	229	−20.54	...	11.8		m
2859	S0	197	−20.96	−20.46	29.3		
2903	Sbc	112[c]	−20.64	...	9.3[d]		
2980	Sbc	170	...	...	...		
2985	Sab	135	−21.35	...	28.6[d]		
3189	...	192	...	...	...		
7177	Sb	128[c]	−20.76	...	28.8[d]		
7457	S0	81[c]	−19.79	...	15.8[d]		
7814	Sab	169	−20.92	...	25.0[d]		

NOTE.—Values of the line strength index γ are given for only the most recent observations. Other observing setups would be on a different scale.

[a] Observed at high dispersion: 22 km s^{-1} bin^{-1}.
[b] From WKS.
[c] Very uncertain since RW has not been determined.
[d] Not a member of a group.
[e] De Vaucouleurs 1958.
[f] Schweizer 1976.
[g] Vorontsov-Vel'yaminov and Savel'eva 1974.
[h] Fraser 1977.
[i] Van Houten 1961.
[j] Blackman 1979.
[k] Tsikoudi 1979.
[l] Burstein 1979*b*.
[m] Assumed bulge magnitude = total magnitude + 0.5.

the observed velocity dispersion for effects of instrumental drifts in wavelength D, and resolution width RW.

$$\sigma_{\text{true}} = [\sigma^2_{\text{observed}} - (0.36D)^2 - \text{RW}^2]^{1/2} \qquad (1)$$

Note that the coefficient for the drift has been adjusted from 0.4 to 0.36 due to subsequent experimentation. The average value of D was 48 km s^{-1}. This correction was insignificant for all but a few galaxies. The resolution width was 100 km s^{-1} for most of the spectra and 36 km s^{-1} for the high resolution spectra. The resulting values of the velocity dispersion are presented in Table 1.

A complicating problem in the recent spectra has been the existence of 12 channel noise. This noise appears to originate in the four-phase readout of the Reticon where our division of each diode into three channels results in a fixed pattern with a periodicity of 12 channels. To mitigate this problem, we first obtain the discrete Fourier transform of the raw spectra and set the value of the transform at the Fourier frequencies corresponding to the 12 channel noise to an average value obtained by averaging 10 channels from each side of this frequency. The spectra are then reconstructed, and the normal procedure is used to obtain velocity dispersions. Numerical tests using spectra which were not contaminated by 12 channel noise indicate that this procedure does not affect the results.

A second set of observations was obtained by Paul Schechter at Mount Hopkins Observatory using their Reticon scanner on the 1.5 m telescope. This second sample of galaxies has several shortcomings: (1) there is very little surface photometry for them. (2) Several galaxies are field galaxies, making distance determinations and hence absolute magnitudes very uncertain. (3) The resolution width has not been determined, making the smaller velocity dispersions very uncertain. These values should therefore be considered as preliminary results. More complete reductions will eventually be performed. Because of these complications, this second set of data will be used in only a limited capacity.

Radial velocities are reported in Table 2. The Fourier quotient method provides an improvement in the accuracy of measuring radial velocities, and in our ability to measure spectra with weak lines and poor signal-to-noise ratios. For example, although seven of our galaxies did not yield reliable velocity dispersions because of weak lines, accurate redshifts were possible. In these cases manual measurements of the radial velocity would have been impossible.

The potential accuracy of our results is determined by the internal uncertainty of the Fourier quotient fit. The average value of this uncertainty was 16 km s^{-1}. Our true uncertainty was much larger, however, due primarily to uncertainties in the wavelength solution, and the correction for the drift in wavelength of the spectrograph, D. This correction was assumed to be $D/2$.

The zero point of our velocity system was determined by using the average of two different calibrations. First, six absorption lines were manually measured for the five template stars. Second, Hβ and λ5007 were measured in emission for seven galaxies. The two separate calibrations gave almost identical results. A further consistency check is possible by comparing our results with the *Second Reference Catalog of Bright Galaxies* (de Vaucouleurs, de Vaucouleurs, and Corwin 1976, hereafter SRC). Using the 36 galaxies we have in common yields a mean difference in the two systems of -22 ± 20 km s^{-1}. However, if our two largest residuals (4536: −207; 4579:

TABLE 2

HELIOCENTRIC RADIAL VELOCITIES

NGC	Radial Velocities (km s^{-1})	Emission Lines	Strength of Emission[a]	Radial Velocities from Emission Lines (km s^{-1})
4189[b]	2069	4861	M	2113
4192	−144	...	...	...
4203	1025	...	...	...
4216	148	...	...	...
4303	1631	4861, 5007	W	1604
4321	1523	...	...	...
4351[b]	2329	4861, 5007	M	2330
4374	924	...	...	...
4382	682	...	...	...
4387	436	...	...	...
4394	730	...	...	...
4406	−279	...	...	...
4413[b]	101	4861, 5007	S	57
4450	1946	...	...	...
4459	1068	...	...	...
4472	903	...	...	...
4478	1363	...	...	...
4486	1371	...	...	...
4519[b]	1038	4861, 5007	W	1076
4535[b]	2018	4861	M	1971
4536[b]	1720	4861, 5007	S	1743
4548	405	...	...	...
4551	1085	...	...	...
4565	1152	...	...	...
4569[b]	−148	...	...	...
4579	1533	...	...	...
4698	998	...	...	...

[a] Line strength: S = strong, M = medium, W = weak.
[b] No measurement of σ.

−272) are discarded, the mean residual becomes -4 ± 17 km s^{-1}.

An estimate of the true uncertainty for independent measurements is possible by comparing our predicted velocities with the true velocities of the template stars. This yields a standard deviation for the residuals of 67 km s^{-1}. A consistency check can be made by noting that our scatter with the SRC is 102 km s^{-1}. The SRC indicates that their average uncertainty in the 26 galaxies we have in common is 76 km s^{-1}. This would leave 68 km s^{-1} for our uncertainty. The agreement of the two methods indicates our uncertainty for an individual measurement is about 70 km s^{-1}.

In the recent set of observations we attempted to measure several galaxies with relatively small bulges to improve our coverage in absolute magnitudes. Unfortunately, most of these galaxies did not yield reliable velocity dispersions because of their weak or nonexistent lines, even when the emission lines were masked from the spectrum. These galaxies are included in Table 2. The weak lines may be partially explained by a decrease in the intrinsic line strength of the spiral bulges as a function of decreasing luminosity, similar to the results for elliptical galaxies (Faber 1973). This interpretation is supported by the study of McClure, Cowley, and Crampton (1980). However, the presence of emission lines in most of these galaxies suggests that the spectra may be contaminated by light from the disk.

III. RESULTS

a) *Velocity Dispersions in Spiral Galaxies:* $L_B \propto \sigma^4$

As shown in WKS, essentially all spiral galaxies have central velocity dispersions which are smaller at a given total luminosity than for elliptical galaxies. This is due to the fact that most of the total luminosity in a spiral galaxy is from the disk component which is supported by the rotational velocities instead of the velocity dispersions. In WKS we show that the velocity dispersions are correlated with the bulge luminosity, with the form $L_B \propto \sigma^4$, similar to the results for elliptical galaxies (Faber and Jackson 1976; Sargent *et al.* 1977; Schechter and Gunn 1979; WKS 1979; Schechter 1980; Terlevich *et al.* 1980; Whitmore 1980).

To obtain the bulge luminosities L_B, we must decompose the observed luminosity profile into contributions from the disk and the bulge. This decomposition was performed using the iterative method suggested by Kormendy (1977). Most of the photometry is from Fraser (1977). Two regions are picked where the bulge and the disk dominate the observed luminosity profile. Data within 3″ are ignored because the limited spatial resolution degrades the steep luminosity gradient in this region. The disk region is then fitted to an exponential profile (Freeman 1970)

$$B = B_c + 1.0857 \Delta r , \quad (2)$$

where B is expressed in blue magnitudes arcsec^{-2}, B_c is the central value of B, and Δ^{-1} is the exponential scale length in arcsec. Galactic extinction is removed in the observed luminosity profile before the fits are made, using 0.2 csc $|b^{\mathrm{II}}|$. The luminosity profile used is a function of an effective radius $r^* \equiv (ab)^{1/2}$, were a and b are the radii of a given isophote along the major and minor axes in arcsec. The disk contribution is then extrapolated into the core and subtracted from the bulge component. The bulge is fitted to a $r^{1/4}$ law (de Vaucouleurs 1948)

$$B = B_e + 8.325[(r/r_e)^{1/4} - 1] , \tag{3}$$

where r_e is the radius containing half of the total luminosity, and B_e is the value of B at this radius. The bulge component is then extrapolated back into the disk region and is subtracted from the disk component. The process is iterated (usually about five times) until a satisfactory fit to both components is obtained. Examples of the resulting fits are shown in Figure 1.

One of the disadvantages of using the $r^{1/4}$ law is that it implies a very rapidly rising luminosity profile in the inner region. For galaxies like NGC 4303, the portion of the $r^{1/4}$ law which is extrapolated inside the first data point at 2″.7 implies a magnitude which is several times the total luminosity of the galaxy. To avoid this problem, excess light above the central surface brightness spuriously required by the $r^{1/4}$ law is removed from the total luminosity.

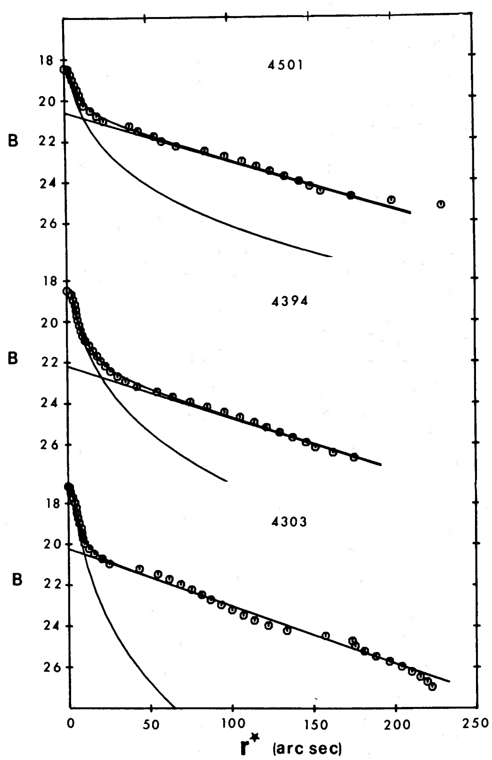

FIG. 1.—Bulge decomposition for NGC 4501 (Sb), NGC 4394 (SBb), and NGC 4303 (Sbc). Surface brightness in blue B (mag arcsec^{-2}) versus effective radius r^*.

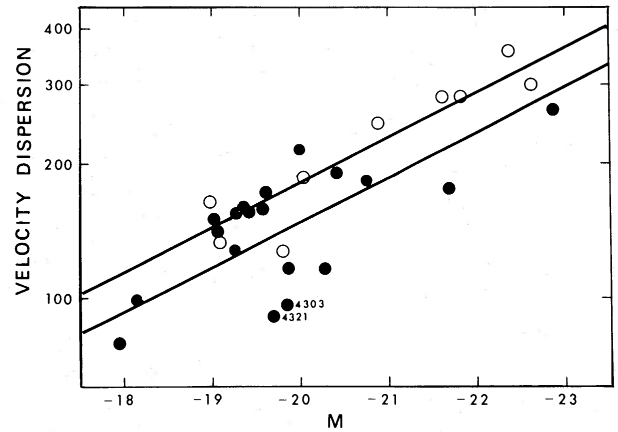

FIG. 2.—Velocity dispersions (km s^{-1}) versus absolute blue magnitude of the spiral bulges and elliptical galaxies. *Open circles*, elliptical galaxies; *filled circles*, spiral bulges. The best-fit lines to the $L \propto \sigma^4$ relation are superposed.

Our adopted bulge magnitudes are presented in Table 1 and plotted versus velocity dispersion in Figure 2. An estimated quality rating (1 = good to 3 = poor) is also included. The best fit line for the 19 spiral bulges yields

$$M = -1.26 + 9.76 \log \sigma . \tag{4}$$

This corresponds to $L_B \propto \sigma^{3.9 \pm 1.1}$. All fits were performed by taking the average of the slopes obtained by performing least squares fits assuming first M, and then log σ, to be the independent parameters. The magnitude system uses B_T magnitudes from the SRC, $H_0 = 50$ km s^{-1} Mpc^{-1}, and galactocentric velocities from group membership (de Vaucouleurs 1975) or the SRC. A cosecant law with a coefficient of 0.2 is used to correct for extinction in our own Galaxy.

The best fit for our nine elliptical galaxies yields

$$M = 2.09 + 8.00 \log \sigma . \tag{5}$$

This gives $L \propto \sigma^{3.2 \pm 0.5}$. The similarity in the relation for the elliptical galaxies and spiral bulges indicates that these systems are dynamically similar. This is consistent with the idea that elliptical galaxies and spiral bulges evolve by the same process. Gott and Thuan (1976) and Larson (1975) have suggested such a scheme, with the fraction of gas remaining after the collapse of the spheroidal component determining the bulge-to-disk ratio.

Previous studies have found a slightly steeper dependence between velocity dispersion and absolute magnitude for elliptical galaxies. Sargent *et al.* (1977) find $L \propto \sigma^{4.0 \pm 1.0}$ for 13 galaxies. Terlevich *et al.* (1980) use 24 ellipticals to obtain $L \propto \sigma^{4.2 \pm 0.2}$. Schechter (1980) simultaneously solves for this relationship and for a Virgocentric velocity and finds $L \propto \sigma^{5.4 \pm 1.0}$. These studies are not particularly good for determining the exact form of this relationship, since the use of field galaxies may cause large uncertainties in the relative distances. The present sample of elliptical galaxies is drawn only from the Virgo cluster and should be free of this problem. However, the small number of galaxies in our sample also dictates a fairly large uncertainty. We conclude that the $L \propto \sigma^4$ relation adequately describes the correlation of both the spiral bulges and the ellipticals, and we adopt this form of the relation for future comparisons. Dynamical explanations for this correlation are developed in Sargent *et al.* (1977), and Aaronson, Huchra, and Mould (1979).

b) The Gap in the $L \propto \sigma^4$ Relations of Spiral Bulges and Elliptical Galaxies

Since we adopt the same $L \propto \sigma^4$ law for both samples, comparisons can be made using the value of the velocity dispersion at a particular absolute magnitude. We employ σ_{21}, the value of σ at $M = -21.0$. A fit to $L \propto \sigma^4$ yields $\sigma_{21} = 190 \pm 10$ km s^{-1} for the spiral bulges and $\sigma_{21} = 228 \pm 11$ km s^{-1} for the ellipticals. This confirms our previous result (WKS) that velocity dispersions are smaller in the spiral bulges (by $17 \pm 8\%$) than in ellipticals at the same absolute magnitude. The standard deviations for the residuals from the $L \propto \sigma^4$ relation are 1.03 mag for the spiral bulges and 0.63 mag for the ellipticals.

Although the difference in σ_{21} appears to be significant, there are several possible systematic errors which could affect our results. To test for possible systematic bias, we have examined several subsets of our sample: using only the spirals with large bulges to avoid disk contamination and measuring errors; using only the Virgo cloud galaxies to minimize distance errors; employing only highly inclined systems to test for disk contamination and rotational effects; and looking only at galaxies that had photometry from a source other than Fraser to test for a possible bias in his data. None of these subsets changes the gap by more than 20%.

A majority of our galaxies use surface photometry from Fraser (1977). Burstein (1979*a*) has shown that this photometry has large scale errors in it. A reassuring fact is that the gap actually increases when galaxies with Fraser's photometry are excluded from the sample.

An independent check on our bulge decompositions is possible using the more accurate photometry and decomposition methods of Boroson (1980). Using his results on 24 spiral galaxies, we can assign an average bulge-to-disk ratio for each Hubble type. Although this introduces scatter since the correlation is not very tight, overall it provides a more accurate test. This procedure does reduce the gap, but only slightly, to 10%.

Although it appears that our results are free of serious systematic biases, the small number of galaxies makes the results tentative. If the gap between the $L \propto \sigma^4$ relation of the spiral bulges and the ellipticals is real, it may be explained as a difference in mass-to-light ratio, central surface brightness, or rotational support (WKS). We are currently involved in a project to obtain velocity dispersions for Boroson's sample. This should allow a more sensitive test of the reality of the gap.

c) The Scatter in the $L \propto \sigma^4$ Relation for Spiral Bulges

Terlevich *et al.* (1980, hereafter TDFB) have argued that much of the scatter in the $L \propto \sigma^4$ relation for elliptical galaxies is not simply the result of observational errors, but is caused by intrinsic differences in these galaxies. The existence of this added parameter was suggested by the fact that the observed scatter is considerably larger than could be explained by the expected uncertainties in σ and M due to uncertainties in the observations. Most authors have argued that this indicated that the estimated uncertainties were too small. TDFB have shown that the quoted uncertainties are actually too large, and the scatter is probably real.

We can make a similar argument for the spiral bulges. The average formal uncertainty in our measurement of σ is 13%, which corresponds to an uncertainty of 0.53 in magnitude. The uncertainty in the measurement of the bulge luminosity is more difficult to estimate, but our experiments with the bulge decompositions suggest that 0.3 mag is a reasonable estimate, though systematic errors in the surface photometry may increase this value. These two uncertainties combine to give a predicted uncertainty of 0.61 mag, well below the value of 1.03 we find in the observed scatter from the $L \propto \sigma^4$ relation. This indicates that much of the scatter is probably real, similar to the case of elliptical galaxies.

We have compared the residuals from the $L_B \propto \sigma^4$ relation in our spiral bulges with several properties of the disk, bulge, and total galaxy [central surface brightness, effective radius of the bulge, morphological type, global color $(B - V)$, rotational velocities, inclination, and line strength index γ]. The only statistically significant correlation we found was with γ. Because of the small number of objects in our sample, it is possible that a weaker correlation with some other property may be obscured by a few discrepant galaxies.

The correlation between the residuals from the $L_B \propto \sigma^4$ relationship for spiral bulges and the line strength index γ is similar to the results of TDFB for elliptical galaxies. However, there are several reasons to remain cautious about the reality of this correlation. The Fourier quotient program indicates that the uncertainties in the determinations of γ and σ are correlated, with a correlation coefficient of about 0.6. This was first pointed out by Schechter and Gunn (1979). Our correlation coefficient is only slightly larger than this (about 0.7), and therefore may be an artifact of the method of measuring dispersions. TDFB have obtained their estimates of line strength by directly measuring the Mg *b* triplet. They argue that this method will circumvent the problem. We have not attempted to obtain line strengths in this way because of the presence of 12 channel noise in our spectrum (see § II). Other reasons for caution are the small number in the sample and the possibility that disk contamination may be important in some of our spectra.

The main conclusion of this section is that the scatter is larger for the spiral bulges than the ellipticals. This indicates that the bulges represent a more heterogeneous sample than the ellipticals. We might expect the spiral bulges to be more heterogeneous because of the possibility of differing degrees of interaction between the bulge and the disk. For example, the presence of gas in the disk may provide the raw material for a burst of star formation which would not be available in an elliptical galaxy. A more accurate description of the situation might be that most of the spiral bulges do fall very close to the line for the ellipticals, and only a few galaxies (perhaps NGC 4303 and NGC 4321 which have the bulges with the steepest luminosity profiles) undergoing a recent burst provide the increased scatter and the gap with the ellipticals.

The increased scatter may also be caused by rotational velocities. If the bulges of spiral galaxies obtain more of their pressure support from rotation, the velocity dispersion can be smaller. Kormendy and Illingworth (1979) have measured absorption line rotation curves in the bulges of three edge-on spiral galaxies. They find peak velocities for the spheroidal components in the range 90–120 km s^{-1}, which they contend are larger than in elliptical galaxies. The bulge of M31 also has a peak velocity in this range (Richstone and Shectman 1979). The average elliptical in a survey of 30 galaxies by Capaccioli (1979) has a peak rotation of about 100 km s^{-1}, when corrected for the random orientation of inclinations. To compare the rotational support properly we must form the ratio V_p/σ, where V_p is the peak rotational velocity. For the four spirals the average value of V_p/σ is 0.57, and for the ellipticals it is 0.42. While the spiral bulges appear to have slightly more rotational support, the small number of observations for spiral bulges makes this result tentative. In particular we note that although NGC 4594 has the largest value of σ, it has the slowest bulge rotation. This suggests that differences in rotational support may produce part of the scatter in the $L_B \propto \sigma^4$ relation. Further observations of the rotation in spiral bulges are clearly needed before we can determine this contribution.

d) *Velocity Dispersions in S0 Galaxies:* $L_B \propto \sigma^4$

We have measured velocity dispersions for 14 S0 galaxies. This represents the first unified sample with enough members to begin studying the correlation between velocity dispersion and absolute bulge luminosity. We shall adopt bulge magnitudes from either Burstein (1979*b*) or Tsikoudi (1977), or we will assume a difference between the total magnitude and the bulge magnitude of 0.50 mag. This is slightly less than the average value for Burstein's S0's (0.84 mag), but his sample is biased toward smaller bulge systems by two effects: (1) Several S0's could not be decomposed because of the lack of a measurable disk. The inclusion of these large bulge systems would lower the average. (2) As Burstein comments, several of these galaxies were selected because of the presence of a large disk component. The value of 0.50 is also in good agreement with the results of Boroson (1980). Our estimates of the bulge magnitudes are reliable despite this crude method because most of the systems are dominated by the bulge, requiring small corrections. To guard against any small bulged S0's such as NGC 4762, we have examined the galaxies on the Palomar Sky Survey, and have subsequently removed NGC 2217 from our sample. NGC 3115 has also been removed because it appears to have a very steep gradient in velocity dispersion which causes large differences in measurements by different authors. For example, Faber and Jackson (1976) find a dispersion of 300 km s^{-1} in the core, but just 160 km s^{-1} at a position 5″ along the major axis. This may indicate the existence of a massive nucleus similar to the one suggested for M87 (Sargent *et al.* 1978), or a rapidly rotating core. The fact that NGC 3115 is not in a group also makes the distance determination, and hence the estimate of L_B, especially uncertain. The S0 bulges are included in Table 1 and plotted in Figure 3. NGC 3115 and NGC 2217 are included in Figure 3, but will be excluded from the following analysis. We note that a value of $\sigma = 160$ km s^{-1} for NGC 3115 would compare favorably with the other S0's,

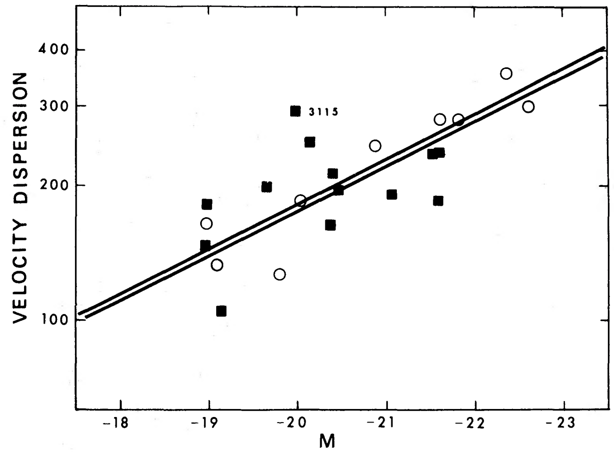

FIG. 3.—Velocity dispersions (km s^{-1}) versus absolute blue magnitude of the S0 bulges and the elliptical galaxies. *Open circles*, elliptical galaxies: *filled squares*, S0 bulges. The best-fit lines to the $L \propto \sigma^4$ relation are superposed, with the fit to the ellipticals higher.

A possible complication in our measurement of σ is the inclusion of four preliminary values from the Mount Hopkins observations. Fortunately, these four galaxies have large enough values of σ to make the lack of a correction for resolution width fairly insignificant (in the worst case a 10% change in σ). The agreement between the four ellipticals we have in common with Schechter (1980), observed using the same system, indicates the two systems are compatible, with a mean difference of 6% (ours being slightly larger) and an average residual of 9%.

The best fit line to our S0's is

$$M = 1.08 + 8.45 \log \sigma , \qquad (6)$$

corresponding to the relationship $L_B \propto \sigma^{3.4 \pm 1.8}$. Although the uncertainty in the exponent is larger than for our spirals or ellipticals, we find that a $L \propto \sigma^4$ relation adequately describes the S0 galaxies. Adopting the $L \propto \sigma^4$ form yields $\sigma_{21} = 220 \pm 15$ km s^{-1}, with a scatter in absolute magnitudes of 0.96 mag. We note that this value of the scatter is between the values found in the ellipticals and spiral bulges. The gap between σ_{21} for the S0's and ellipticals is 4 ± 8%. The fact that the $L \propto \sigma^4$ relation holds for the spheroidal components of spiral, S0, and elliptical galaxies provides evidence that these systems are dynamically similar (though the possible gap between σ_{21} for the spiral bulges and ellipticals suggests that they may not be identical).

IV. THE DYNAMICS OF SPIRAL GALAXIES

a) Comparison of Velocity Dispersions with Rotational Velocities

If the spheroidal bulge is the dominant massive component in a spiral galaxy, both the velocity dispersion and the rotational velocities in the disk will be determined by the same potential. As demonstrated by Gott (1977), the collisionless Boltzmann equation then leads to

$$V_R{}^2(r) = -\sigma^2(r)\frac{d \ln \rho_B(r)}{d \ln r}, \tag{7}$$

where V_R is the rotational velocity in the disk at a galactocentric radius r, and $\rho_B(r)$ is the density of the bulge at this radius. This equation assumes an isotropic velocity dispersion and no rotation in the bulge. If we approximate the density profile as $\rho_B(r) \propto r^{-\alpha}$ in the outer regions of the galaxy, then equation (7) becomes

$$V_A/\sigma = (\alpha)^{1/2}, \tag{8}$$

where V_A is the asymptotic rotational velocity reached in the outer parts of the rotation curve. The flat rotation curves observed by Krumm and Salpeter (1979) and by Rubin, Ford, and Thonnard (1978) imply $\alpha = 2$. We therefore expect a value of about 1.4 for the ratio of V_A/σ for spirals with dominant bulge components.

We have estimated values of V_A by using neutral hydrogen widths. We estimate V_A by dividing the H I widths by 2 sin i, where i is the inclination determined using the procedure of Heidmann, Heidmann, and de Vaucouleurs (1971) and axial ratios from the SRC. Values of V_A/σ are presented in Table 3 and plotted versus L_B/L_T in Figure 4, where L_T is the total luminosity.

Several of our galaxies cannot be directly included in Figure 4 because we have no estimate of L_B/L_T. However,

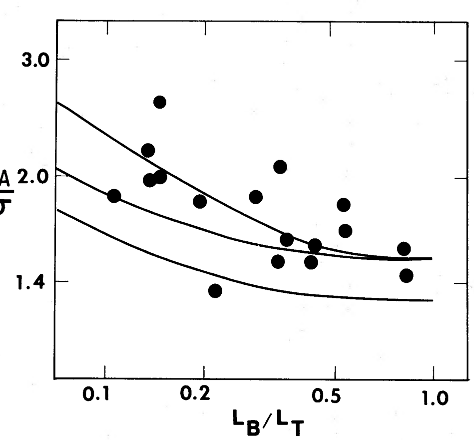

FIG. 4.—Ratio of asymptotic velocities to velocity dispersion V_A/σ versus the ratio of bulge luminosity to total luminosity L_B/L_T. The bottom curve (model 1) is the basic model with only a bulge and disk. The middle curve (model 2) is with rotational support. The top curve (model 3) is with rotational support and a massive halo.

we note that the two S0a galaxies have low values of V_A/σ (1.50 for NGC 2655 and 1.20 for NGC 3593). We also find that the two Sc galaxies in the preliminary Mount Hopkins sample reinforce the trend toward higher values of V_A/σ for small bulge systems (2.83 for NGC 628 and 2.28 for NGC 1084). We have not included NGC 5457 (Scd) in our sample because it is almost face-on, making an estimate of the rotational velocity very uncertain. However, for any reasonable value of the rotational velocity V_A/σ will be about 3.0.

A least-squares fit to the data gives

$$\log\left(\frac{L_B}{L_T}\right) = 0.41 - (3.82 \pm 1.26) \log\left(\frac{V_A}{\sigma}\right). \tag{9}$$

Note that for a system dominated by the bulge with $\log (L_B/L_T) = 0$, $V_A/\sigma = 1.28$. This is probably an underestimate, since there is some evidence in the data that the slope of the correlation is flatter for large bulge systems. If we consider only the galaxies with $L_B/L_T > 0.4$, the average value of this ratio becomes $V_A/\sigma = 1.60 \pm 0.06$. This is an overestimate, since these galaxies are not totally dominated by the bulge. We find that our data are compatible with the prediction from equation (8) that V_A/σ is equal to 1.41 for totally bulge dominated galaxies.

The agreement with the prediction could stem from various sources. The mass may be in a spheroidal halo that has a $\rho \propto r^{-2}$ distribution, as suggested in our discussion of equation (8). This spheroidal mass distribution may just be the extension of the visible bulge, or it may be a distinct component. Another possibility is that spirals may have massive thin disks. In this case the velocity dispersion of the bulge would be a response to the potential of the disk, rather than the main support mechanism. In other words, the role of V_A and σ would be reversed from the massive spheriod picture.

The major problem with the thin disk model is that the bulge does not appear to be dominated by the disk. Instead, it is very likely that the bulge controls the rotation curve of the disk in the inner regions. Spirals with small bulges have shallow velocity gradients while spirals with large bulges have steep gradients. In the case of the three best resolved spirals with sizable bulges (M31, Rubin and Ford 1970; M81, Goad 1976; and our own Galaxy, Burton and Gordon 1978) the gradient near the center is extremely steep, and the curves show a distinct inner peak at about 1 kpc. The inner peak is almost certainly caused by the bulge. This indicates that the bulge is the dominant massive component in the central region at least, and is therefore decoupled from any hypothetical massive thin disk.

A possible objection that could be raised by proponents of a massive disk is that while the inner region may be dominated by the spheroidal component, it is still possible that the outer region is dominated by the disk. In this case the agreement of our data with the prediction from equation (8) must be viewed as a coincidence, since there is no coupling mechanism between V_A and σ. Other studies which favor a spheriod over a disk are the isophotes of bulges (Monet, Richstone, and Schechter

TABLE 3

NEUTRAL HYDROGEN WIDTHS

NGC	Type	H I Width (km s^{-1})	Source[a]	i (°)	Corrected H I Width (km s^{-1})	V_A/σ	L_B/L_T
			Spirals				
224	Sb	538	1, 2	72	566	1.87	0.283
3031	Sab	445	1, 3	58	525	1.67	0.535
3351	SBb	278	2, 3	47	380	1.88	0.105
4192	Sab	455	1	74	473	1.85	0.191
4254	Sc	283	4	27	623	1.98	0.137
4303	Sbc	178	3, 5	25	421	2.19	0.134
4321	Sbc	272	4, 5	35[b]	474	2.60	0.141
4394	SBb	193	4	25	457	1.62	0.353
4450	Sab	341	2, 3	45	482	2.08	0.337
4501	Sb	532	1, 4	57	634	1.99	0.143
4548	SBb	246	4	36	419	1.35	0.215
4579	Sb	356	2	36	606	1.59	0.433
4594	Sa	750	6	84[c]	754	1.43	0.817
4698	Sab	428	3, 4	56	516	1.50	0.425
7217	Sab	359	7	32	677	1.83	0.525
7331	Sbc	522	2, 5	70	556	1.58	0.809
4203	S0	274	8	30[d]	548	1.50	0.334
			Galaxies without Values of L_b/L_T				
488	Sb	456	3	40	709	1.51	
628	Sc	122	5	21	340	2.83	
681	Sab	386	3	51	497	1.79	
1084	Sc	356	3, 5	58	420	2.28	
2336	Sbc	474	3, 5	56	572	2.03	
2655[e]	S0a	265	2	33	487	1.50	
2841	Sb	604	3	64	672	1.47	
3368[e]	Sab	354	2, 3	45	501	2.18	
3593[e]	S0a	260	2, 9	68	280	1.20	
3623[e]	Sa	514	3, 9	75	532	1.78	
3627[e]	Sb	386	3	61	441	1.20	
3628[e]	Sb	490	3	80	498	1.42	
4378	Sa	351	9	22	937	2.86	
4725[e]	Sab	414	2, 3	45	585	1.76	
4736[e]	Sab	242	2	34	433	1.62	
7814	Sab	455	8	68	491	1.45	

[a] SOURCE.—(1) Tully and Fisher 1977, measured at 20% intensity. (2) WKS 1979, 25%. (3) Dickel and Rood 1978, 25%. (4) Sandage and Tammann 1976, 20%. (5) Shostak 1978, 20%. (6) Faber *et al.* 1977, 25%. (7) Rubin *et al.* 1978. (8) Krumm, private communication, 25%. (9) Krumm and Salpeter 1978, 50%.

[b] Van der Kruit 1973.

[c] From Sandage 1961.

[d] Krumm, private communication.

[e] WKS.

1981) and the stability of warped disks (Tubbs and Sanders 1979). As we shall show in § IV*b*, the data in Figure 4 can be naturally explained by the massive spheroid model.

Returning to the spheriod model, we note that Figure 4 can help distinguish between the case where the massive halo is an extension of the bulge, and the case where it is a distinct component. We find that the small bulged spirals have a higher value of V_A/σ than the bulge dominated galaxies. This indicates that for the later type spirals, the halo is not an extension of the bulge. If so, we would expect the velocity dispersion in both the halo and bulge to be approximately equal. The value of V_A/σ would then be about 1.4 for all spiral galaxies, not just the bulge dominated ones. We conclude that the bulge and halo are dynamically distinct in these systems. This was first shown in WKS.

Recently Frenk and White (1980) have reexamined the globular cluster system in our own Galaxy. They find that the velocity dispersion in the central region is 96 km s^{-1}, while in the outer region the dispersion is 133 km s^{-1}. This result again suggests that the inner and outer regions of the spheroidal component are decoupled. It also may indicate that the inner globular clusters are related to the bulge while the outer clusters are related to the halo.

Another reason for suggesting that the bulge and halo are dynamically distinct for later type galaxies is the inner peak in well resolved rotation curves at about 1 kpc. The rapid decline in the rotational velocities just beyond this peak implies a rapid falloff in the density profile of the bulge, and ensure that the bulge is not the cause of the flat rotation curve in the outer region. A prediction of our model is that for large bulged systems which appear to be more closely related to the outer halo, this decline in the rotation curve should be less pronounced or nonexistent.

One final argument is that if the bulges themselves make the rotation curves flat, the gradient in M/L must be very steep since the light distribution goes as about $r^{-2.8}$ (Spinrad, Ostriker, and Stone 1978) while the mass goes as r^{-2}. The lack of a correspondingly strong color gradient suggests that the dark halo material and the luminous bulge material are from very different populations and may therefore have had different histories.

b) *A Three-Component Model for Spiral Galaxies*

Although we have discussed the large and small bulge systems separately, there is actually a continuum of spirals with intermediate sized bulges. Our data suggest that this is also a continuum of how dynamically distinct the bulge and halo are. For the early spirals the bulge and halo appear to be closely related, while in the later spirals they appear to be distinct. We have constructed a simple three-component model to help fill in this continuum, and to aid in the interpretation of Figure 4. For the bulge component we adopt a King (1966) model with $\log(r_t/r_c) = 2.1$, where r_t is the tidal radius and r_c is the core radius. A program written by Brian Flannery was used to generate this component. The disk is a Freeman (1970) exponential disk. For the halo we use an isothermal sphere, since the flat rotation curves indicate that $\rho \propto r^{-2}$, as is the case for an isothermal velocity distribution. The models are a simple superposition of these three components. This superposition represents a major approximation in our model since we would expect each component to readjust its mass distributions in response to the potential of the other components. A more self-consistent model will be developed in the future. For the present, we find that our simple model is useful for demonstrating the gross dynamical features of spiral galaxies.

Each component has three parameters: the central mass density, the characteristic radius (r_c for the bulge and halo, Δ for the disk; see eq. [2]), and the mass-to-light ratio (assumed constant throughout each component). The M/L ratio in the halo is actually superfluous since the only constraint is that the halo be unobservable with current techniques. This occurs for M/L ratios over about 100. We therefore have eight parameters in our models. The models determine the rotation curve in the disk, the velocity dispersion profile in the bulge and halo, and the luminosity profile. In addition, a global H I profile is determined by assuming the density profile of the hydrogen in the disk, and a velocity dispersion in the gas of 10 km s^{-1}. Bosma (1978) has shown that beyond about 10 kpc the ratio of the mass density to H I density is constant. Inside 10 kpc the ratio appears to rise linearly, indicating that the fraction of the disk which is gas is decreasing. Using Bosma's results, we adopt a density profile for the gas proportional to $\rho_D(0)\ 10^{-0.12(10-r)}$ from $r = 0$ kpc to $r = 10$ kpc, after which point it remains constant. The quantity $\rho_D(0)$ is the central mass density in the disk. With the further assumption that the inclination of the galaxy is 45°, we are able to integrate over the entire galaxy and produce global H I profiles for our model galaxies. These are useful for comparing with H I observations.

We adopt values for M/L of 3 for the disk, 8 for the bulge, and 200 for the halo. These values are representative of estimates of M/L: (1) in the solar neighborhood for the disk, (2) in ellipticals, S0's, and Sa's for the bulge, and (3) in large clusters of galaxies for the halos (Faber and Gallagher 1979). A reassuring fact is that our preliminary M/L ratios for the bulge component of Boroson's (1980) galaxies average about 9. For the characteristic radii we shall adopt $\Delta = 2500$ pc for the disk, and $r_c = 10{,}000$ pc for the halo. The core radius of the bulge is varied from 50 to 500 pc to produce galaxies with different bulge-to-disk ratios. This ratio could also be varied by changing other parameters such as the central mass density of the bulge or disk, the M/L of the bulge or disk, or R_c of the disk. While these parameters are certainly not completely independent of the bulge-to-disk ratio, our photometry indicates that a change in r_c of the bulge is the dominant variable which determines L_B/L_T. In a future paper, individual models will be made for each of Boroson's galaxies. The estimate of r_c for the halo is very uncertain. The values for the bulge and disk are representative of most normal spirals (Freeman 1970; Ostriker and Caldwell 1979). The central mass densities are 500 $M_\odot$ pc^{-2} (corresponding to a central surface brightness of 21.5 mag arcsec^{-2}) in the disk, 133 $M_\odot$ pc^{-3} in the bulge, and 0.0132 $M_\odot$ pc^{-3} in the halo. Figure 5 shows an example of the resulting kinematic and photometric profiles from a model with $r_c = 150$ pc in the bulge. This particular model most closely resembles an Sab galaxy. The closest match to one of our galaxies might be NGC 4394.

Values of V_A are taken at the 25% intensity level of the H I widths, and corrected to edge-on. Our first set of models (model 1) produce the bottom curve in Figure 4. This set of models has no halo. We find that the slope becomes flatter for the bulge dominated systems. This is a plausible result because for the large bulges, both V_A and σ are determined by the bulge component and the assumptions in equation (8) are approximately satisfied. In the small bulge region V_A is determined mainly by the disk, and therefore remains fairly constant while σ decreases.

The most interesting facet of model 1 is that it falls well below most of our data points. It is likely that part of this shift is due to rotational support, which our models have not explicitly considered. This would allow σ to be smaller and could account for the discrepancy. We can include this contribution approximately by using equation (10) which follows from the discussion of Young *et al.* (1978):

$$\frac{M(r)}{r} \propto V_A{}^2 + \alpha\sigma_{\rm cor}{}^2 . \qquad (10)$$

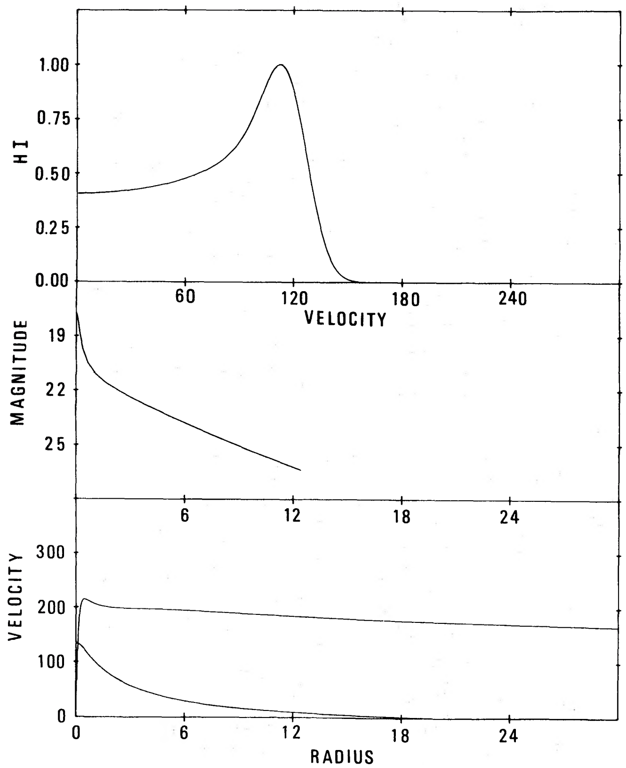

FIG. 5.—Kinematic and photometric profiles for a typical three-component model. The bottom panel shows the rotation curve (*upper curve*) and the velocity dispersion curve in the bulge. The middle panel shows the luminosity profile. The top panel shows the H I profile. Velocities are in km s^{-1}; the radius is in kpc. This is a model 3 galaxy with $r_c = 150$ pc for the bulge. It has $L_B/L_T = 0.38$ and $V_A/\sigma = 1.64$ (corrected for bulge rotation).

Here $\sigma_{\rm cor}$ is the value of σ corrected for the rotational support. Previously we had assumed $V_A = 0$ km s^{-1} in equation (10), giving $M(r)/r \propto \alpha\sigma^2$. Combining this equation with equation (10) yields

$$\frac{\sigma_{\rm cor}}{\sigma} = \left[1 - \frac{1}{\alpha}\left(\frac{V_A}{\sigma}\right)^2\right]^{1/2} . \tag{11}$$

We shall adopt a value of 2.5 for α. This is the value of $d \ln \rho / d \ln r$ in the region of interest for a King model with $\log (r_t/r_c) = 2.1$. We also need to correct our value of $V_A/\sigma = 0.57$ adopted for spiral bulges (§ IIIc) for line-of-sight projection effects. Young *et al.* indicate that this would increase V_A/σ by about 37%, to $V_C/\sigma = 0.78$ for spiral bulges. Using these estimates in equation (11) indicates that $\sigma_{\rm cor}/\sigma = 0.87$. The central curve in Figure 4 is identical to model 1 except that the correction for rotational support has been included (model 2). Although this removes some of the discrepancy between our model and the observations, the agreement is still very poor.

The agreement is improved greatly by including a massive halo. The top curve in Figure 4 (model 3) is identical to model 2 except a moderately massive halo has been added. We find much better agreement between this model and the observations. In this model, 14% of the mass inside 5 kpc is from the halo, while 58% is from the bulge and 28% is from the disk. These values are for a typical galaxy with $L_B/L_T = 0.38$, as shown in Figure 5. We have picked 5 kpc as a fiducial because it represents a position in the model which is fairly similar to our position in our Galaxy, though it should be kept in mind that this model is more appropriate for a slightly small Sab galaxy than for a giant Sbc (de Vaucouleurs 1979). The local mass density at 5 kpc is 0.12 $M_\odot$ pc^{-3} for the disk component (assuming an exponential scale height in the disk of 300 pc) and 0.02 $M_\odot$ pc^{-3} for the spheroidal component (consisting mainly of the halo at this distance).

Although the models are only approximate and must be modified to be made self-consistent, we believe that these results suggest the presence of a massive halo for most spiral galaxies, of the type suggested by Ostriker, Peebles, and Yahil (1974). A massive halo has also been invoked to explain the observations of flat rotation curves at large galactic radii (Bosma 1978; Krumm and Salpeter 1979; Rubin, Ford, and Thonnard 1978). Studies of clusters of galaxies and galaxy pairs have also been used to suggest the presence of this unseen mass (see Faber and Gallagher 1979 for several references). Our results provide independent evidence for the existence of this component.

In the future it should be possible to reduce the observational scatter considerably. The determination of L_B/L_T is again a major concern. The measurement of core radii in the bulge will also be important since it will allow us to obtain estimates of M/L in the bulge directly. Our models would then provide a very useful approach for studying the global properties of spiral galaxies, especially the structural properties of the halo.

This approach is more direct than the disk stability arguments and is on firmer observational ground than the studies of binaries and clusters, which may be dominated by selection effects. While the observations of flat rotation curves still provide the best evidence for the existence of an unseen massive component, these rotation curves cannot distinguish between a massive disk and a massive spheroid. Models using both rotational velocities and velocity dispersions should help determine the detailed mass distribution of this extra mass.

V. SUMMARY

Central velocity dispersions have been obtained for a large sample of elliptical, S0, and spiral galaxies to establish the following results.

1. We have confirmed the finding by WKS that the $L \propto \sigma^4$ relation that holds for elliptical galaxies is applicable to the spiral bulges, but with velocity dispersions which are 17 ± 8% smaller at the same absolute magnitude. Difficulties in obtaining the bulge magnitudes and the possibility of other systematic errors may affect this gap. The similarity in this relationship between elliptical galaxies and spiral bulges indicate that the systems are dynamically similar and suggests that they may have similar histories.

2. The scatter from the $L_B \propto \sigma^4$ relation is con-

siderably larger in the spiral bulges than in the ellipticals. The scatter in the S0 galaxies is intermediate. It appears that part of the scatter for the spiral bulges is due to the heterogeneity of the spiral bulges.

3. The bulges of S0 galaxies follow the same $L_B \propto \sigma^4$ relation as elliptical galaxies. This offers further evidence for the similarity of the spheroidal component of elliptical, S0, and spiral galaxies.

4. We have compared our central velocity dispersions with rotational velocities obtained by using global neutral hydrogen widths. We find a significant decrease in the ratio of V_A/σ for galaxies with smaller bulges. This indicates that the bulge and the halo are dynamically separate components.

5. Our data also supports the prediction that $V_A/\sigma = 1.4$ for bulge dominated systems. This suggests that the unseen mass which causes rotation curves to remain flat resides in a spheroid rather than a thin disk.

6. A simple three-component model for a spiral galaxy has been developed to aid in the analysis. A comparison of these models with the data suggests the presence of a massive halo. Further observations should reduce the scatter in the V_A/σ versus L_B/L_T relation, allowing these models to be useful for determining several global properties of spiral galaxies.

We would like to thank Paul Schechter for making the observations at Mount Hopkins and for several helpful discussions and suggestions. Discussions with Jeremiah Ostriker were also very helpful. The King models were generated using a program generously lent to us by Brian Flannery. We would also like to thank Matt Johns and Chris Price for support of the instrumentation at McGraw-Hill, and the Research Corporation for their help in providing the TV guider. R. P. K. acknowledges the generous support of the Alfred P. Sloan Foundation. B. C. W. was partially supported by a Horace H. Rackham Fellowship.

REFERENCES

Aaronson, M., Huchra, J., and Mould, J. 1979, *Ap. J.*, **229**, 1.
Blackman, C. P. 1978, *M.N.R.A.S.*, **186**, 717.
Boroson, T. 1980, thesis, University of Arizona.
Bosma, A. 1978, thesis, University of Groningen.
Burstein, D. 1979*a*, *Ap. J. Suppl.*, **41**, 435.
———. 1979*b*, *Ap. J.*, **234**, 435.
Burton, W. B., and Gordon, M. A. 1978, *Astr. Ap.*, **63**, 7.
Capaccioli, M. 1979, in *Photometry, Kinematics, and Dynamics of Galaxies*, ed. D. S. Evans (Austin: University of Texas at Austin/Dept. of Astronomy), p. 165.
de Vaucouleurs, G. 1948, *Ann. d'Ap.*, **11**, 247.
———. 1958, *Ap. J.*, **128**, 465.
———. 1975, in *Galaxies and the Universe*, ed. A. Sandage, M. Sandage, and J. Kristian (Chicago: University of Chicago Press), p. 557.
———. 1979, in *IAU Symposium 84, The Large Scale Characteristics of the Galaxy*, ed. W. B. Burton (Dordrecht: Reidel), p. 203.
de Vaucouleurs, G., de Vaucouleurs, A., and Corwin, H. G. 1976, *Second Reference Catalogue of Bright Galaxies* (Austin: University of Texas Press) (SRC).
Dickel, J. R., and Rood, H. J. 1978, *Ap. J.*, **223**, 391.
Faber, S. M. 1973, *Ap. J.*, **179**, 731.
Faber, S. M., Balik, B., Gallagher, J. S., and Knapp, G. R. 1977, *Ap. J.*, **214**, 383.
Faber, S. M., and Gallagher, J. S. 1979, *Ann. Rev. Astr. Ap.*, **17**, 135.
Faber, S. M., and Jackson, R. E. 1976, *Ap. J.*, **204**, 668.
Fraser, C. W. 1977, *Astr. Ap. Suppl.*, **29**, 161.
Freeman, K. C. 1970, *Ap. J.*, **160**, 811.
Frenck, C. S., and White, S. D. M. 1980, *M.N.R.A.S.*, **193**, 295.
Goad, J. W. 1976, *Ap. J. Suppl.*, **32**, 89.
Gott, J. R., III. 1977, *Ann. Rev. Astr. Ap.*, **15**, 235.
Gott, J. R., and Thuan, T. X. 1976, *Ap. J.*, **204**, 649.
Heidmann, J., Heidmann, N., and de Vaucouleurs, G. 1971, *Mem. R.A.S.*, **75**, 85.
King, I. R. 1966, *A.J.*, **71**, 64.
Kormendy, J. 1977, *Ap. J.*, **217**, 406.
Kormendy, J., and Illingworth, G. 1979, in *Photometry, Kinematics, and Dynamics of Galaxies*, ed. D. S. Evans (Austin: University of Texas at Austin/Dept. of Astronomy), p. 195.
Krumm, N., and Salpeter, E. E. 1979, *Ap. J.*, **228**, 64.
Larson, R. B. 1975, *M.N.R.A.S.*, **173**, 671.
McClure, R. D., Cowley, A. P., and Crampton, D. 1980, *Ap. J.*, **236**, 112.
Monet, D., Richstone, D. O., and Schechter, P. L. 1981, *Ap. J.*, **245**, 454.
Ostriker, J. P., and Caldwell, J. A. R., in *IAU Symposium 84, The Large Scale Characteristics of the Galaxy*, ed. W. B. Burton (Dordrecht: Reidel), p. 441.
Ostriker, J. P., Peebles, P. J. E., and Yahil, A. 1974, *Ap. J.* (*Letters*), **193**, L1.
Richstone, D. O., and Shectman, S. A. 1979, *Ap. J.*, **235**, 30.
Rubin, V. C., and Ford, W. K. 1970, *Ap. J.*, **159**, 379.
Rubin, V. C., Ford, W. K., and Thonnard, N. 1978, *Ap. J.* (*Letters*), **225**, L107.
Sandage, A. 1961, *The Hubble Atlas of Galaxies* (Washington: Carnegie Institution).
Sandage, A., and Tammann, G. A. 1976, *Ap. J.*, **210**, 7.
Sargent, W. L. W., Schechter, P. L., Boksenberg, A., and Shortridge, K. 1977, *Ap. J.*, **212**, 326.
Sargent, W. L. W., Young, P. J., Boksenberg, A., Shortridge, K., Lynds, C. R., and Hartwick, F. D. A. 1978, *Ap. J.*, **221**, 731.
Schechter, P. L. 1980, *A.J.*, **85**, 801.
Schechter, P. L., and Gunn, J. E. 1979, *Ap. J.*, **229**, 472.
Schweizer, F. 1976, *Ap. J. Suppl.*, **31**, 313.
Shostak, G. S. 1978, *Astr. Ap.*, **68**, 321.
Spinrad, H., Ostriker, J. P., and Stone, R. P. S. 1978, *Ap. J.*, **225**, 56.
Terlevich, R., Davies, R. L., Faber, S. M., and Burstein, D. 1980, preprint (TDFB).
Tsikoudi, V. 1979, *Ap. J.*, **234**, 842.
Tubbs, A. D., and Sanders, R. H. 1979, *Ap. J.*, **230**, 736.
Tully, R. G., and Fisher, J. R. 1977, *Astron. Ap.*, **54**, 661.
van der Kruit, P. C. 1973, *Ap. J.*, **186**, 805.
van Houten, C. J. 1961, *Bull. Astr. Inst. Netherlands*, **16**, 1.
Vorontsov-Vel'yaminov, B. A., and Savel'eva, M. V. 1974, *Soviet Astr.*, **17**, 643.
Whitmore, B. C. 1980, *Ap. J.*, **242**, 53.
Whitmore, B. C., Kirshner, R. P., and Schechter, P. L. 1979, *Ap. J.*, **234**, 68 (WKS).
Young, P., Sargent, W. L. W., Boksenberg, A., Lynds, C. R., and Hartwick, F. D. A. 1978, *Ap. J.*, **222**, 450.

ROBERT P. KIRSHNER: Department of Astronomy, University of Michigan, Ann Arbor, MI 48109

BRADLEY C. WHITMORE: Department of Terrestrial Magnetism, Carnegie Institution of Washington, 5241 Broad Branch Road, N.W., Washington, DC 20015